Journal of Physics: Conference Series **676** (2016) 012001 doi:10.1088/1742-6596/676/1/012001

An exact formulation of *k*-distribution methods in non-uniform gaseous media and its approximate treatment within the Multi-Spectral framework

Frédéric ANDRE[1,3], Longfeng HOU[1], Vladimir P. SOLOVJOV[2]

[1] Université de Lyon, CNRS, INSA-Lyon, CETHIL, UMR5008, F-69621 Villeurbanne, France
[2] Brigham Young University, Department of Mechanical Engineering, CTB 435, Provo, UT 84602,USA

E-mail: frederic.andre@insa-lyon.fr

Abstract. The main restriction of *k*-distribution approaches for applications in radiative heat transfer in gaseous media arises from the use of a scaling or correlation assumption to treat non-uniform situations. It is shown that those cases can be handled exactly by using a multidimensional *k*-distribution that addresses the problem of spectral correlations without using any simplifying assumptions. Nevertheless, the approach cannot be suggested for engineering applications due to its computational cost. Accordingly, a more efficient method, based on the so-called Multi-Spectral Framework, is proposed to approximate the previous exact formulation. The model is assessed against reference LBL calculations and shown to outperform usual *k*-distribution approaches for radiative heat transfer in non-uniform media.

1. Introduction

Radiative heat transfer in gaseous media is encountered in many engineering and research studies dedicated, for instance, to the effect of radiation on the structures of planetary atmospheres or for the calculation of heat fluxes at the walls of combustion chambers. The most accurate and flexible model to treat gas radiation interactions is the so-called Line-By-Line (LBL) approach. LBL spectra are based directly on spectroscopic databases and provide gas radiative properties at high resolution. Nevertheless, this method is computationally too expensive to be used in many situations. For most engineering applications, simpler models are required.

Many approximate methods have been proposed during the past decades to treat radiative heat transfer in gaseous media. A compendium of the existing ones can be found for instance in Refs. [1,2]. Among them, *k*-distribution techniques are currently the most widely used, partly due to their ability to be applied together with any Radiative Transfer Equation (RTE) solver. They are usually accurate and can be readily extended to any band width, from narrow bands up to the Full Spectrum (FS), with minor modifications. The so-called ADF [3], FSK [4] and SLW [5] models are undoubtedly the most famous FS *k*-distribution approaches and have been applied to many engineering configurations. Over narrow bands, the C*k* (Correlated-*k*) [1] model is recognized as one of the most relevant choices to treat gas radiation. All those models are essentially based on the same set of two equations (the first one for the *k*-distribution formulation in uniform media and the second one for its extension to non-

[3] To whom any correspondence should be addressed.

uniform cases – this second equation is usually based on a scaling or correlated assumption of gas spectra in distinct thermophysical states). Those models provide good accuracy for most engineering applications but may fail to give reliable results when high temperature gradients are encountered along the radiation path. This is mainly due to the appearance of "hot lines" (at high temperature) that are missing in the gas spectra at low temperatures. The effect of these lines is to break the "ideal" behaviour of the gas spectra and may reduce drastically the accuracy of the approximate models based on this assumption. This problem (encountered for instance in IR plume signature, or in some emission spectroscopy configurations) can be solved by application of the so-called fictitious gases approach [6] or by using mapping techniques [7,8]. Those methods improve the accuracy of the approximate model but usually at the cost of a large increase in terms of computational resources.

The aim of the present paper is to show that *k*-distributions can be formulated exactly in non-uniform media by replacing the usual *k*-distribution concept (that is defined for a given thermophysical state) by a multidimensional one. Using this exact model in engineering applications cannot be suggested in a general frame but approximate solutions can be proposed. The method to approximate this exact solution for radiative transfer applications was described in a previous paper and led us to develop the so-called "Multi-Spectral Framework - MSF" [8]. It will be shown that all existing models are special cases of the MSF. This point is raised in Section 4. Results obtained through the application of this technique are assessed against reference LBL calculations in situations representative of engineering problems, in 0D (along line-of-sights) and 1D (plane parallel walls) geometries.

2. *k*-distribution methods

k-distribution approaches were introduced in 1934 by Ambartzumian [9]. At this time, due to a lack of information about the real profiles of spectral lines, the absorption coefficient was assumed to be a periodic function of the wavelength. The same technique was used to treat real gas spectra (without any name but with reference to Ambartzumian's work) during the following decades (see for instance Refs. [10,11]). The name "*k*-distribution" only appeared (to our knowledge) in 1972 [12]. Since then, many papers have been devoted to its application both in uniform (homogeneous isothermal) and non-uniform media [1,2].

In these methods, the (narrow) band averaged transmission function of a path of length L inside a gas at a uniform temperature T, pressure P, and molar fraction in absorbing specie x is expressed as:

$$\tau^{\Delta\eta}(L) = \frac{1}{\Delta\eta}\int_{\Delta\eta}\exp\left(-xP\kappa_\eta L\right)\,d\eta \;=\; \int_0^{+\infty}\exp\left(-xPLk\right)\,f(k)\,dk \tag{1}$$

where $f(k)$ is the *k*-distribution function. For any real interval $[k,k+dk]$, $dk>0$, $f(k)\,dk$ represents the fraction of wavenumbers $\eta\in\Delta\eta$ such that the value of the spectral absorption coefficient of the gas is inside the interval $[k,k+dk]$. Eq. (1) can also be written in terms of the cumulative distribution of *k*-values, $g(k)$, as:

$$\tau^{\Delta\eta}(L) = \int_0^{+\infty} exp\left(-xPLk\right)\,dg(k) \tag{2}$$

Eq. (2) mainly consists of a change of variable of integration $\eta\leftrightarrow k$ (or equivalently $\eta\leftrightarrow g(k)$ as g is strictly monotonous). Therefore, it provides the exact band averaged transmission function. The main source of error arises in practice from the use of numerical quadratures to estimate this integral. Mathematically, $g(k)$ associates to any value of $k\in\mathbb{R}$ a probability to find a value of κ_η lower than k inside $\Delta\eta$. This probability $\mathbb{P}$ is defined as the fraction of the interval $\Delta\eta$ such that $\kappa_\eta<k$. It can be written formally as [1]:

$$\mathbb{P}\left(\kappa_\eta < k, \eta \in \Delta\eta\right) = g(k) = \frac{1}{\Delta\eta}\int_{\Delta\eta} H\left(k-\kappa_\eta\right) d\eta \;\Leftrightarrow\; f(k) = \frac{dg(k)}{dk} = \frac{1}{\Delta\eta}\int_{\Delta\eta} \delta\left(k-\kappa_\eta\right) d\eta \qquad (3)$$

In Eq. (3), H is the Heaviside function and δ is the Dirac delta function defined as [13] (where F is any continuous function defined over the real axis and c is a constant):

$$\delta(x-c) = 0,\ x \neq c \qquad (4)$$

$$\int_{-\infty}^{+\infty} \delta(x-c)\, F(x)\, dx = F(c) \qquad (5)$$

The notation used in the second term at the RHS in Eq. (3) is purely formal. In fact, "function" $\delta\left(k-\kappa_\eta\right)$ is mathematically defined only if the absorption coefficient is strictly monotonous over the interval (viz. if the derivative of the absorption coefficient with respect to the wavenumber does not vanish, [13]) which is not the case in a general frame. Furthermore, this definition of the distribution function only has a sense inside an integral over k (such as in Eq. (1)). Accordingly, in the present paper, as soon as possible, equations will make use of g, which defines a measure on the spaces of k-values and that can be written in terms of Heaviside function as shown in Eq. (3), rather than f. Nevertheless, as this notation is usual in gas radiation, we will make use of $\delta\left(k-\kappa_\eta\right)$ in the paper. Consequently, all spectral bands must be understood as the restrictions of the intervals over which $\delta\left(k-\kappa_\eta\right)$ is mathematically defined. As the number of minima and maxima of the absorption coefficient are always finite inside a spectral interval, the values of the spectral integrals are not changed if we consider the full band or those restricted sets of wavenumbers.

k-distribution approaches can be extended to non-uniform media by assuming "ideal" behaviours of the variations of the absorption coefficient with respect to the thermophysical conditions. The most widely used assumptions are called the scaling and correlation approximations [14]. They are briefly described in the next section.

3. Multidimensional *k*-distribution methods in non-uniform media

3.1. Preliminary comments

In this section, we introduce the method proposed to extend k-distribution approaches used in uniform media to non-uniform ones. The technique is detailed in a simple case where the path is discretized in two uniform sub-paths in distinct thermophysical states. The approach is then extended to the general case where the non-uniform path can be divided into $n \in \mathbb{N}$ homogeneous isothermal elements. Furthermore, the only kind of path non-uniformity considered here will be due to temperature. This is not a limitation of the method, as it can also be applied when gradients of composition or pressure are encountered along the path, but this assumption is made to simplify the notations.

Only spectral narrow bands will be considered in this work.

3.2. Exact treatment of spectral correlation effects

Let us consider a narrow spectral interval $\Delta\eta$ that: 1/ is narrow enough to assume that the Planck function remains constant, 2/ do not contain any transparency region of the gas at any temperature (this means that $\forall \eta \in \Delta\eta,\ \forall T \in \left[T_{\min}, T_{\max}\right],\ \kappa_\eta(T) > 0$ where $T_{\min}$ and $T_{\max}$ represent the minimum and maximum temperatures encountered along the non-uniform path).

Over band $\Delta\eta$, it is possible to exhibit relationship between absorption coefficients $\kappa_\eta(T_1)$ and $\kappa_\eta(T_2)$ at two distinct temperatures, $T_1 \neq T_2$ arbitrarily chosen inside the interval $\left[T_{\min}, T_{\max}\right]$, by plotting one of them (for instance $\kappa_\eta(T_2)$) as a function of the other one (in this case $\kappa_\eta(T_1)$). This

approach provides a 2-dimensional parametric curve $k_1 = \kappa_\eta(T_1)$, $k_2 = \kappa_\eta(T_2)$ in the (k_1, k_2)-plane, that will be subsequently referred to as the *C* curve. This curve can be interpreted in the following way:

- If *C* is a straight line $k_2 = U \cdot k_1$ with $U > 0$, then for any wavenumber $\eta \in \Delta\eta$ we have $\kappa_\eta(T_2) = U \cdot \kappa_\eta(T_1)$, and then the two absorption coefficients are called scaled.
- If *C* is a function $k_2 = F(k_1)$, then for any value of $\eta \in \Delta\eta$, we have $\kappa_\eta(T_2) = F\left[\kappa_\eta(T_1)\right]$ and the two absorption coefficients are correlated. It should be noticed that in the literature on gas radiation, the concept of correlation usually involved is more restrictive since it assumes *F* to be strictly monotonous [1].

In other cases, no conclusion about correlation can be made: generally, when absorption coefficients associated to two distinct temperatures are plotted as a function of each other, none of the two previous situations (viz. scaling or correlation) is rigorously encountered.

To illustrate this fact, we consider the two spectra plotted in figure 1. They correspond to two absorption coefficients given by the Elsasser model (infinite array of regularly spaced identical Lorentz lines). As those absorption coefficients are assumed to be associated to distinct thermophysical states, spectra in figure 1 were obtained by using distinct values of the Half Widths at Half Maximum (HWHM) of the Lorentz profiles (to account for the effect of pressure, composition and temperature changes between the two states) as well as of the line intensity (known to be strongly temperature dependent). Furthermore, the distance between lines was chosen distinct in the two spectra to account for the possible appearance of "hot" lines. The corresponding parametric curve *C*, based on the previous absorption coefficients, is shown in figure 2.

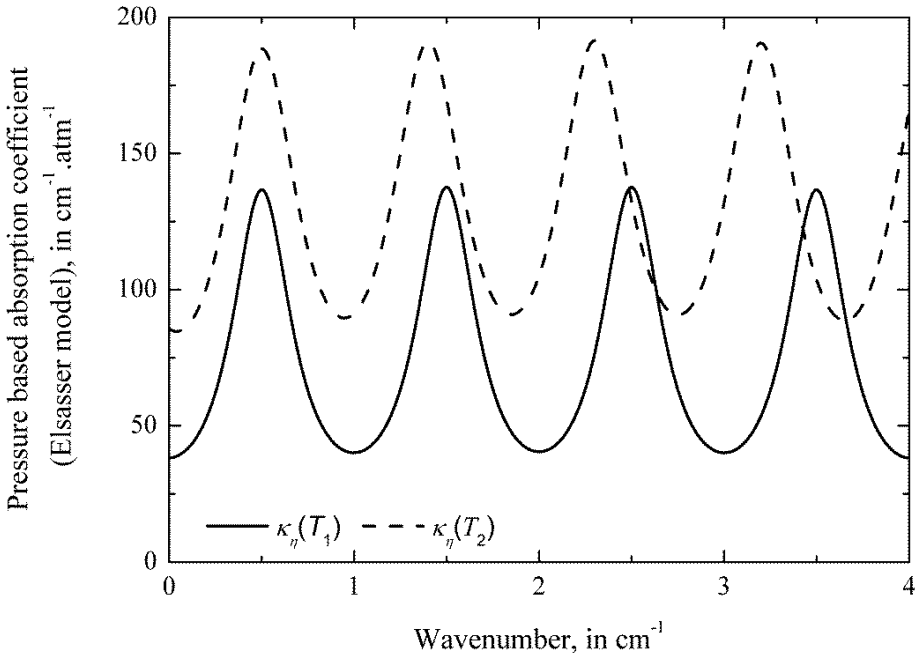

Figure 1. Elsasser model of absorption coefficients at two distinct thermophysical states.

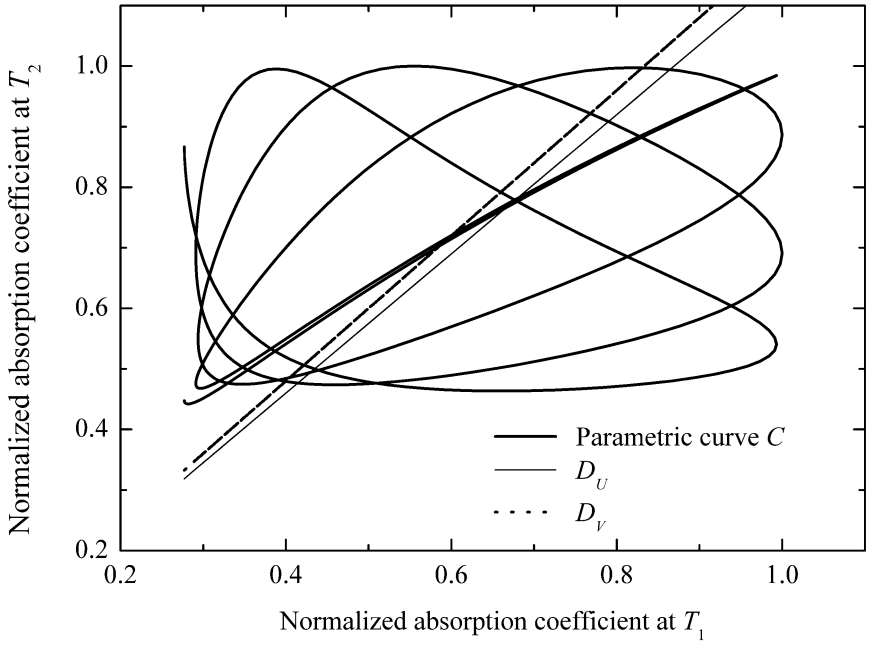

Figure 2. Parametric curve *C* for the two absorption spectra depicted in figure 1.

Our objective is to calculate the mean value of some continuous real valued function *F* of both $\kappa_\eta(T_1)$ and $\kappa_\eta(T_2)$ averaged over band $\Delta\eta$:

$$F^{\Delta\eta} = \frac{1}{\Delta\eta}\int_{\Delta\eta} F\left[\kappa_\eta(T_1),\kappa_\eta(T_2)\right] d\eta \tag{6}$$

As $\kappa_\eta(T_1)$ and $\kappa_\eta(T_2)$ are neither scaled nor correlated, it is not easy to suggest a simple method to handle the calculation of this integral. One possible technique is described below.

Let us introduce two straight lines, that will be called D_U and D_V, whose equations are given respectively as $k_2 = U\cdot k_1$ and $k_2 = V\cdot k_1$ with $V > U > 0$ (see figure 2). Any point on curve *C* with coordinates $\left(k_1=\kappa_\eta(T_1),\ k_2=\kappa_\eta(T_2)\right)$ located between D_U and D_V is such that:

$$U < \kappa_\eta(T_2)/\kappa_\eta(T_1) < V \tag{7}$$

or equivalently:

$$U < u_\eta(T_1,T_2) < V \tag{8}$$

where we define the function $u_\eta(T_1,T_2) = \kappa_\eta(T_2)/\kappa_\eta(T_1)$ to represent the spectral scaling function between the two absorption spectra.

The fraction of the interval $\Delta\eta$ for which Eqs. (7,8) are satisfied is:

$$\frac{\Delta\eta(U,V)}{\Delta\eta} = \frac{1}{\Delta\eta}\int_U^V \left\{\int_{\Delta\eta}\delta\left[u-u_\eta(T_1,T_2)\right] d\eta\right\} du \tag{9}$$

and the mean value of function *F* over the same set of wavenumbers is given as:

$$F^{\Delta\eta(U,V)} = \int_U^V \left\{ \frac{1}{\Delta\eta(U,V)} \int_{\Delta\eta} \delta\left[u - u_\eta(T_1,T_2)\right] \; F\left[\kappa_\eta(T_1),\kappa_\eta(T_2)\right] d\eta \right\} du \tag{10}$$

Since variables η and u are independent, the following (purely formal) equality:

$$\int_{\Delta\eta} \delta\left[u - u_\eta(T_1,T_2)\right] F\left[\kappa_\eta(T_1),\kappa_\eta(T_1)\cdot u_\eta(T_1,T_2)\right] d\eta = \int_{\Delta\eta} \delta\left[u - u_\eta(T_1,T_2)\right] F\left[\kappa_\eta(T_1),u\cdot\kappa_\eta(T_1)\right] d\eta \tag{11}$$

enables to write Eq. (10) as:

$$F^{\Delta\eta(U,V)} = \frac{1}{\Delta\eta(U,V)} \int_{\Delta\eta} \left\{ \int_U^V \delta\left[u - u_\eta(T_1,T_2)\right] F\left[\kappa_\eta(T_1),u\cdot\kappa_\eta(T_1)\right] du \right\} d\eta \tag{12}$$

Now, we observe that:

$$\lim_{\substack{U\to 0 \\ V\to+\infty}} \Delta\eta(U,V) = \Delta\eta \tag{13}$$

Eq. (13) simply means that when $U \to 0$, then D_U approaches the k_1-axis, and if $V \to +\infty$, then D_V approaches the k_2-axis. In this case, the domain between the two lines covers the first quarter of the real plane, to which any value of $\kappa_\eta(T_1)$ and $\kappa_\eta(T_2)$ belong.

Using Eq. (13), we can then conclude that:

$$\lim_{\substack{U\to 0 \\ V\to+\infty}} F^{\Delta\eta(U,V)} = F^{\Delta\eta} = \frac{1}{\Delta\eta} \int_{\Delta\eta} \left\{ \int_0^{+\infty} \delta\left[u - u_\eta(T_1,T_2)\right] F\left[\kappa_\eta(T_1),u\cdot\kappa_\eta(T_1)\right] du \right\} d\eta \tag{14}$$

The previous equation can also be written by using the property of the Delta function given by Eq. (5) that provides $F\left[\kappa_\eta(T_1),u\cdot\kappa_\eta(T_1)\right] = \int_0^{+\infty} \delta\left[k - \kappa_\eta(T_1)\right] F(k,u\cdot k)\, dk$:

$$F^{\Delta\eta} = \int_0^{+\infty}\int_0^{+\infty} \left\{ \frac{1}{\Delta\eta} \int_{\Delta\eta} \delta\left[u - u_\eta(T_1,T_2)\right] \delta\left[k - \kappa_\eta(T_1)\right] d\eta \right\} F(k,u\cdot k)\, dk\, du \tag{15}$$

Eq. (15) can then be reformulated using the change of variables $k_1 = k$, $k_2 = u\cdot k$. Indeed, the Jacobian corresponding to this change of variable is k (which is strictly positive, as assumed in section 3.2) and, using Eq. (21) page 53 from Ref. [13], we can write formally here: $\delta\left[u - u_\eta(T_1,T_2)\right]\cdot\delta\left[k - \kappa_\eta(T_1)\right] = k\cdot\delta\left[k_1 - \kappa_\eta(T_1)\right]\cdot\delta\left[k_2 - \kappa_\eta(T_2)\right]$. This provides

$$F^{\Delta\eta} = \int_0^{+\infty}\int_0^{+\infty} \left\{ \frac{1}{\Delta\eta} \int_{\Delta\eta} \delta\left[k_1 - \kappa_\eta(T_1)\right] \delta\left[k_2 - \kappa_\eta(T_2)\right] d\eta \right\} F(k_1,k_2)\, dk_1\, dk_2 \tag{16}$$

This equation generalizes the usual *k*-distribution approach given by Eq. (1) to non-uniform media. Indeed, the previous relation can be written as:

$$F^{\Delta\eta} = \int_0^{+\infty}\int_0^{+\infty} F(k_1,k_2)\, dg(k_1,k_2) \tag{17}$$

in which we have introduced the 2-dimensional cumulated *k*-distribution:

$$g(k_1,k_2)=\frac{1}{\Delta\eta}\int_{\Delta\eta} H\left[k_1-\kappa_\eta(T_1)\right]\,H\left[k_2-\kappa_\eta(T_2)\right]\,d\eta \tag{18}$$

It should be noticed that, as in the case of *k*-distribution methods for uniform media, using distribution $g(k_1,k_2)$ provides an exact value of the spectral average of $F\left[\kappa_\eta(T_1),\kappa_\eta(T_2)\right]$ over $\Delta\eta$. Now, let us consider the particular case:

$$F\left[\kappa_\eta(T_1),\kappa_\eta(T_2)\right]=exp\left[-x_1P_1\;\kappa_\eta(T_1)L_1-x_2P_2\;\kappa_\eta(T_2)L_2\right] \tag{19}$$

where L_1 and L_2 are the lengths of two uniform columns at temperature T_1 and T_2, compositions x_i, $i=1,2$ and total pressures P_i, $i=1,2$ respectively. $F^{\Delta\eta}$ represents in this case the band averaged transmission function $\tau^{\Delta\eta}(L)$ of a non-uniform path $L=L_1+L_2$. Application of Eq. (17) to this function enables to calculate exactly the transmissivity of the non-uniform path.

Furthermore, Eq. (17) remains exact not only for this non-uniform case but also for uniform situations (at temperature T_1 or T_2 that are particular cases of Eq. (17) with L_1 = 0 or L_2 = 0). In fact, in these situations, Eq. (17) simplifies to the usual *k*-distribution model. Additionally, it is worth noticing that the exactness of the approach does not rely on assumptions of scaling or correlation about gas spectra, which are known to be the main source of error for the application of *k*-distribution techniques in non-uniform media.

The simple process that we have described in this section for the treatment of a non-uniform gas path at two distinct temperatures can be readily applied to real gas spectra (instead of the Elsasser model, as considered previously). An example of the parametric curve *C* in a real case is given in figure 3. It corresponds to two spectra of H_2O over the [3287.5 ; 3292.5] cm^{-1} spectral interval for T_1 = 300 K and T_2 = 2,300 K – additional details about the LBL data used for the curve are given in the caption to figure 3.

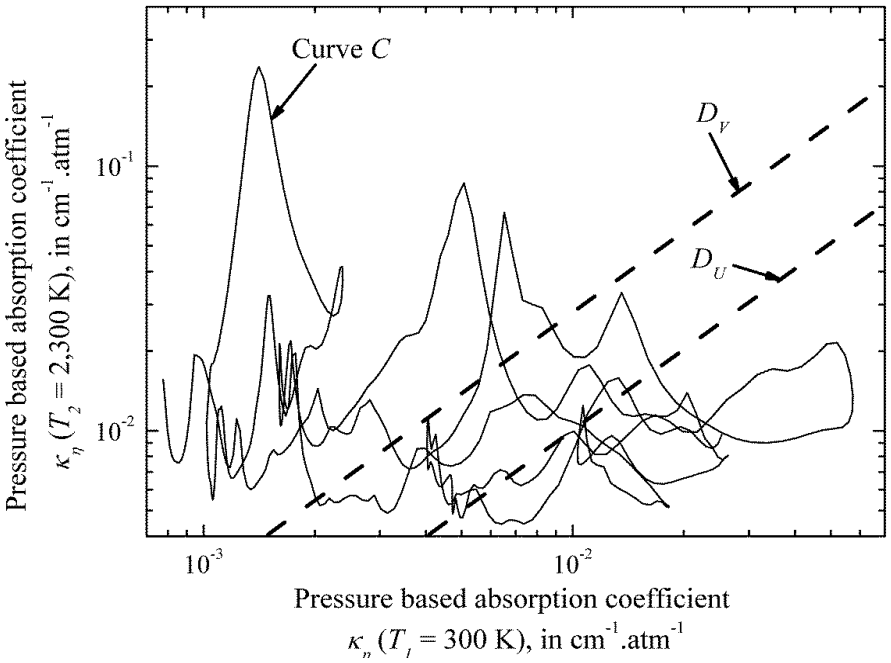

Figure 3. Parametric curve *C* representing $\kappa_\eta(T_2)$ as a function of $\kappa_\eta(T_1)$ for H_2O at T_1 = 300 K and T_2 = 2,300 K – 10% of H_2O with 90% N_2 – values of κ_η are considered over the [3287.5 ; 3292.5] cm^{-1} spectral interval.

Clearly, since curve *C* is not monotonous, the two spectra are neither scaled nor correlated. Notice that in log-log scales, as used on this figure, lines D_U and D_V are parallel with a slope of 1. The constant distance between D_U and D_V is $ln(V/U)$.

The approach can also be generalized to calculate band averaged values of functions *F* of any set of distinct temperatures $\{T_1,T_2,..,T_n\}$ where n is the number of isothermal sub-layers encountered along the non-uniform path. The method is then fundamentally the same as the one given in this section (but then parametric curves *C* in dimensions higher than 2 have to be considered). This provides, as a generalization of Eqs. (17,18):

$$\begin{aligned} F^{\Delta\eta} &= \frac{1}{\Delta\eta}\int_{\Delta\eta} F\left[\kappa_\eta(T_1),\kappa_\eta(T_2),..,\kappa_\eta(T_n)\right] d\eta \\ &= \underbrace{\int_0^{+\infty}\int_0^{+\infty}...\int_0^{+\infty}}_{n \text{ integrals}} F(k_1,k_2,..,k_n)\; dg_n(k_1,k_2,..,k_n) \end{aligned} \tag{20}$$

where the *n*-dimensional cumulated *k*-distribution is defined as:

$$g_n(k_1,k_2,..,k_n) = \frac{1}{\Delta\eta}\int_{\Delta\eta} H\left[k_1-\kappa_\eta(T_1)\right] H\left[k_2-\kappa_\eta(T_2)\right]...H\left[k_n-\kappa_\eta(T_n)\right] d\eta \tag{21}$$

Eq. (20) can also be written in a simpler form by introducing the vector $\boldsymbol{k}=(k_1,\ k_2,\ ..,\ k_n)\in\mathbb{R}_+^n$:

$$F^{\Delta\eta} = \int_{\boldsymbol{k}\in\mathbb{R}_+^n} F(\boldsymbol{k})\; dg_n(\boldsymbol{k}) \tag{22}$$

together with the following notations:

$$g_n(\boldsymbol{k}) = g_n(k_1,k_2,..,k_n) \tag{23-a}$$

$$F(\boldsymbol{k}) = F(k_1,k_2,..,k_n) \tag{23-b}$$

One of the main advantages of the last formulation is that it is formally the same as encountered in usual *k*-distribution approaches. Eq. (22) may also be extended from discrete to continuous temperature distributions along a non-uniform path using a functional integral form as shown in Appendix.

Finally, the presented method is not restricted to non-uniformities in terms of temperature but can also be applied in cases of gradients of pressure or species concentrations. This enables to write formally Eq. (21) in a more general form:

$$g_n(k_1,k_2,..,k_n) = \frac{1}{\Delta\eta}\int_{\Delta\eta} H\left[k_1-\kappa_\eta(\underline{\phi}_1)\right] H\left[k_2-\kappa_\eta(\underline{\phi}_2)\right]...H\left[k_n-\kappa_\eta(\underline{\phi}_n)\right] d\eta \tag{24}$$

where $\underline{\phi}_i$, $i=1,..,n$ represent the state vectors whose components are the gas temperatures, total pressures, and species concentration encountered along the non-uniform path.

4. The Multi-Spectral Framework (MSF).

4.1. Principle of the MSF

One of the main problems for the application of Eq. (22) for radiative heat transfer is that it requires to estimate the multidimensional cumulative *k*-distribution $g_n(\boldsymbol{k})=g(k_1,k_2,..,k_n)$, which can be computationally expensive if n is large. However, this approach can be considered in some cases (see

for instance Ref. [7], in which a similar process is applied in the context of radiative transfer in the atmosphere). Nevertheless, a more efficient method is required for most engineering applications. One of them is the so-called Multi-Spectral Framework (MSF) introduced in Ref. [8]. It is out of the scope of the present work to provide a comprehensive description of this approach, and more detail can be found in Ref. [8].

In the MSF, the first step is to consider a particular case of Eq. (22) in which temperatures $\{T_1,..,T_n\}$ are chosen distinct and regularly spaced between $T_{\min}$ and $T_{\max}$: $T_{\min}=T_1<T_2<...<T_n=T_{\max}$. In the second step, it is assumed that it is possible to define P distinct and linearly independent continuous scaling functions $u_p(T)$, $p=1,..,P$ such that for any wavenumber $\eta\in\Delta\eta$, one can find an integer $p\in\{1,..,P\}$ such that:

$$\forall i\in\{1,..,n\},\ \kappa_\eta(T_i)=\kappa_\eta\left(T^{ref}\right)\ u_p(T_i) \tag{25}$$

where T^{ref} represents a reference temperature, chosen arbitrarily inside the interval $[T_{\min},T_{\max}]$. Here, we choose the reference temperature $T^{ref}=T_1$, that implies: $u_p(T_1)=1$. Eq. (25) allows definition of P spectral subintervals $\Delta\eta(u_p)$, $p=1,..,P$: $\bigcup_{p=1,P}\Delta\eta(u_p)=\Delta\eta$ that can be used to discretize Eq. (22) into:

$$F^{\Delta\eta}=\frac{1}{\Delta\eta}\sum_{p=1}^{P}\Delta\eta(u_p)\cdot\int_{\boldsymbol{k}\in\mathbb{R}_+^n}F(\boldsymbol{k})\ dg_{n,p}(\boldsymbol{k}) \tag{26}$$

where, as a direct application of Eq. (21):

$$g_{n,p}(\boldsymbol{k})=\frac{1}{\Delta\eta(u_p)}\int_{\Delta\eta(u_p)}H\left[k_1-\kappa_\eta(T_1)\right]H\left[k_2-\kappa_\eta(T_2)\right]...H\left[k_n-\kappa_\eta(T_n)\right]\,d\eta \tag{27}$$

and where $\Delta\eta(u_p)$ is the width of the spectral interval set by Eq. (25).

It can be noticed that it is always possible to define such a finite set of scaling functions because in practice LBL data are calculated at limited resolution (which means that inside an interval, the number *N* of spectral values of the absorption coefficient is finite and the number of distinct scaling functions is utmost equal to *N*). Then, the third step consists in using the definition of the scaling functions given by Eq. (25) inside Eq. (27) to set:

$$g_{n,p}(\boldsymbol{k})=\frac{1}{\Delta\eta(u_p)}\int_{\Delta\eta(u_p)}H\left[k_1-\kappa_\eta\left(T^{ref}\right)\right]H\left[k_2-\kappa_\eta\left(T^{ref}\right)\cdot u_p(T_2)\right]...H\left[k_n-\kappa_\eta\left(T^{ref}\right)\cdot u_p(T_n)\right]\,d\eta \tag{28}$$

It can be shown (see Eq. (27) in Ref. [8]) that Eq. (28) simplifies into:

$$g_{n,p}(\boldsymbol{k})=\frac{1}{\Delta\eta(u_p)}\int_{\Delta\eta(u_p)}H\left[k_1-\kappa_\eta\left(T^{ref}\right)\right]\,d\eta=g_p\left(k_1,T^{ref}\right) \tag{29}$$

where $g_p\left(k_1,T^{ref}\right)$ is the distribution of *k*-values at the reference temperature $T^{ref}=T_1$ inside the interval $\Delta\eta(u_p)$.

Accordingly, Eq. (26) can be written in a very simple form (see Eq. (26) in Ref. [8]):

$$F^{\Delta\eta}=\frac{1}{\Delta\eta}\sum_{p=1}^{P}\Delta\eta(u_p)\int_0^{+\infty}F\left[k_1,k_1\cdot u_p(T_2),..,k_1\cdot u_p(T_n)\right]dg_p\left(k_1,T^{ref}\right) \tag{30}$$

The application of the MSF thus reduces the calculation of a multidimensional *k*-distribution to a weighted sum of usual ones. Furthermore, for any spectrum of the gas at a temperature $T \in [T_{\min}, T_{\max}]$, it is possible to approximate $\kappa_\eta(T)$ over any spectral interval $\Delta\eta(u_p)$, $p = 1,..,P$ as:

$$\kappa_\eta(T) \approx \kappa_\eta(T_1) \cdot u_p(T), \ \eta \in \Delta\eta(u_p) \tag{31}$$

This provides, for instance for the transmission function of the gas at temperature T:

$$\tau^{\Delta\eta}(L) = \frac{1}{\Delta\eta} \int_{\Delta\eta} exp\left[-xP\kappa_\eta(T)L\right] d\eta \approx \frac{1}{\Delta\eta} \sum_{p=1}^{P} \Delta\eta(u_p) \int_0^{+\infty} exp\left[-xP\, k_1 \cdot u_p(T)\, L\right] dg_p(k_1, T^{ref}) \tag{32}$$

Obviously, this approach can also be extended to non-uniform paths.
The main difficulty for the application of the previous equations is the definition of the set of scaling functions $u_p(T)$, $p = 1,..,P$. This point is raised in the next section.

4.2. Application of a functional clustering technique to define $\Delta\eta(u_p)$, $p = 1,..,P$

Let us consider an arbitrary integer $p \in \{1,..,P\}$ and two arbitrary distinct wavenumbers $\eta_1, \eta_2 \in \Delta\eta(u_p)$. Following the definition of intervals $\Delta\eta(u_p)$ (see Eq. (25)), we have:

$$C(\eta_1, \eta_2) = \int_{T_{\min}}^{T_{\max}} \kappa_{\eta_1}(T)\kappa_{\eta_2}(T)dT = \kappa_{\eta_1}(T^{ref})\kappa_{\eta_2}(T^{ref}) \int_{T_{\min}}^{T_{\max}} \left[u_p(T)\right]^2 dT \tag{33}$$

and:

$$C(\eta_1, \eta_1)C(\eta_2, \eta_2) = \int_{T_{\min}}^{T_{\max}} \left[\kappa_{\eta_1}(T)\right]^2 dT \int_{T_{\min}}^{T_{\max}} \left[\kappa_{\eta_2}(T)\right]^2 dT = \left[\kappa_{\eta_1}(T^{ref})\kappa_{\eta_2}(T^{ref})\right]^2 \left\{\int_{T_{\min}}^{T_{\max}} \left[u_p(T)\right]^2 dT\right\}^2 \tag{34}$$

that shows that:

$$\frac{C(\eta_1, \eta_2)}{\left[C(\eta_1, \eta_1)C(\eta_2, \eta_2)\right]^{1/2}} = 1 \tag{35}$$

Similarly, if the two wavenumbers are chosen in distinct spectral intervals $\Delta\eta(u_p)$ and $\Delta\eta(u_{p'})$, $p \neq p'$ then, according to the Cauchy-Schwartz inequality [15]:

$$0 \leq \frac{C(\eta_1, \eta_2)}{\left[C(\eta_1, \eta_1)C(\eta_2, \eta_2)\right]^{1/2}} = \frac{\int_{T_{\min}}^{T_{\max}} u_p(T)u_{p'}(T)dT}{\left\{\int_{T_{\min}}^{T_{\max}} \left[u_p(T)\right]^2 dT\right\}^{1/2} \left\{\int_{T_{\min}}^{T_{\max}} \left[u_{p'}(T)\right]^2 dT\right\}^{1/2}} < 1 \tag{36}$$

Consequently, the two criteria set by Eqs. (35,36) can be used to group together the wavenumbers that have the same scaling functions and thus to determine the spectral intervals $\Delta\eta(u_p)$. This process is usually referred to as Functional Data Clustering [16], which is a part of more general Functional Data Analysis (FDA) [17].

FDA is a relatively new area of mathematical science whose aim is to extend the usual techniques encountered for Multivariate Statistical Analysis (MSA) of data (such as clustering techniques for instance) to functions. The steps for Functional Data Clustering are [18]:

1/ Propose a functional form for the data.

2/ Estimate the parameters that provide the best estimate of the data using the functional form chosen in the previous step.

3/ Calculate a similarity (see Eq. (35)) or a distance between functions based on integrals (and not in terms of distances between points, which is the most significant difference between FDA and MSA).

4/ Apply usual techniques encountered in MSA (such as clustering, principal component analysis, etc) using the coefficients of similarities (or distances) obtained at the previous stage to build groups (here spectral intervals) associated to similar functions.

Table 1 summarizes the two functional forms of the scaling function (step 1) considered in this work. The first one was used previously in Ref. [8]. It can be shown that the two formulas given in the third column converge toward their exact value (see Eq. (37)) when $T_i \to T_{i+1}$.

Table 1. Functional forms used for the definition of the similarity coefficient required in the clustering process and associated cross-correlation coefficients over $[T_i, T_{i+1}]$, $T_i \in \{T_1,..,T_n\}$.

Functional Form	Approximation of $\ln\left[u_\eta(T)/u_\eta(T_i)\right]$ over an interval $[T_i, T_{i+1}]$, α is a coefficient	$C_{i,i+1}(\eta_1,\eta_2)$ (see Eq. (37)) Spectral scaling functions $u_{\eta_j}(T)$, j = 1,2 are defined here as: $u_{\eta_j}(T) = \kappa_{\eta_j}(T)\left\{\int_{T_{\min}}^{T_{\max}} \left[\kappa_{\eta_j}(T')\right]^2 dT'\right\}^{-1/2}$
FF1	$\alpha(T - T_i)$	$\dfrac{u_{\eta_1}(T_{i+1})u_{\eta_2}(T_{i+1}) - u_{\eta_1}(T_i)u_{\eta_2}(T_i)}{\ln\left[u_{\eta_1}(T_{i+1})u_{\eta_2}(T_{i+1})\right] - \ln\left[u_{\eta_1}(T_i)u_{\eta_2}(T_i)\right]}(T_{i+1} - T_i)$
FF2	$\alpha \ln(T/T_i)$	$\dfrac{u_{\eta_1}(T_i)u_{\eta_2}(T_i)T_i}{\alpha_{\eta_1} + \alpha_{\eta_2} + 1}\left[\left(\dfrac{T_{i+1}}{T_i}\right)^{\alpha_{\eta_1}+\alpha_{\eta_2}+1} - 1\right]$, $\alpha_{\eta_j} = \dfrac{\ln\left[u_{\eta_j}(T_{i+1})/u_{\eta_j}(T_i)\right]}{\ln(T_{i+1}/T_i)}$

The third column in table 1 enables to calculate the correlation coefficients that appear in Eqs. (35,36) as (for instance for $C(\eta_1,\eta_2)$, and omitting the product $\kappa_{\eta_1}(T^{ref})\kappa_{\eta_2}(T^{ref})$ for simplicity):

$$C(\eta_1,\eta_2) = \int_{T_{\min}}^{T_{\max}} u_{\eta_1}(T)u_{\eta_2}(T)dT = \sum_{i=1}^{n-1}\left[\int_{T_i}^{T_{i+1}} u_{\eta_1}(T)u_{\eta_2}(T)dT\right] = \sum_{i=1}^{n-1} C_{i,i+1}(\eta_1,\eta_2) \qquad (37)$$

Those coefficients can be used in Eqs. (35,36) to evaluate the similarity (in terms of scaling functions) between any couple of wavenumbers. The wavenumbers associated to the highest values of this coefficient can then be grouped into clusters (here we have used a hierarchical clustering based on an average linkage scheme [16] – this method was shown in Ref. [19] to be well suited for the clustering of functional data). Once clusters are built, we have groups of wavenumbers that share similar scaling functions. The width $\Delta\eta\left(u_p\right)$ of the corresponding spectral interval can be estimated as $\Delta\eta\left(u_p\right)=N_p\ \delta\eta$ where N_p represents the number of elements in the *p*-th cluster (the one associated to the *p*-th scaling function $u_p\left(T\right)$) and $\delta\eta$ is the distance (assumed constant over $\Delta\eta$) between two successive values of the absorption coefficients in the LBL dataset.

4.3. Approximate treatment of non-uniformities over clusters

Following the method described in the previous subsection to build spectral intervals $\Delta\eta\left(u_p\right),\ p=1,..,P$, the most natural way to evaluate the radiative properties of the gas over each cluster of wavenumbers is by using a Scaled-*k* approach. The main problem is that over those clusters, absorption coefficients are not rigorously scaled, but only share similar behaviors (in other words, the application of a clustering technique only ensures that the elements that are inside a same cluster are more similar with respect to the coefficients given by Eqs. (35,36) than those that are outside this cluster). This is shown in figure 4. As a consequence, functions $\hat{u}_p\left(\underline{\phi}\right)=u_p\left(T\right)\cdot u_p^{'}\left(x,P\right)$, where $\hat{u}_p\left(\underline{\phi}\right)$ represents the scaling function between states $\underline{\phi}^{ref}$ and $\underline{\phi}$ and $u_p^{'}\left(x,P\right)$ is the part of the function related to composition and pressure, cannot be defined explicitly but only implicitly as a solution of the following implicit equation [14] (over each interval $\Delta\eta\left(u_p\right)$):

$$\int_0^{+\infty} exp\left(-xPkL\right)\ dg_p\left(k,\underline{\phi}\right)=\int_0^{+\infty} exp\left[-x^{ref}P^{ref}k^{ref}L\ \hat{u}_p\left(\underline{\phi}\right)\right]\ dg_p\left(k^{ref},\underline{\phi}^{ref}\right) \qquad (38)$$

where $g_p\left(k,\underline{\phi}\right)$ is the cumulative distribution of values of *k* in the thermophysical state $\underline{\phi}=\{\ x,\ P,\ T\ \}$ over the interval $\Delta\eta\left(u_p\right)$ and $\underline{\phi}^{ref}$ represents a prescribed reference thermophysical state. It can be shown easily that the previous equation does not provide a solution that only changes with the thermophysical state of the gas but that it also depends on the length of the path considered in Eq. (38). This means that this equation needs to be solved iteratively along the propagation of the radiation inside the gaseous medium, which is not convenient for applications in radiative heat transfer.

In order to circumvent this difficulty, we notice that as over clusters absorption coefficients are mostly linearly correlated, the use of the correlation assumption is here justified. Accordingly, instead of equation (38), we define, for convenience, the absorption coefficient $k\left(\underline{\phi}\right)$ in any state $\underline{\phi}$ as a solution of the well known correlation equation [1], whose application is fully justified here because the correlating function is strictly increasing (since $\hat{u}_p\left(\underline{\phi}\right)>0$):

$$g_p\left(k,\underline{\phi}\right)=g_p\left(k^{ref},\underline{\phi}^{ref}\right) \qquad (39)$$

Using this method, the local absorption coefficients can be calculated once and then stored in tables. Other practical advantages of this treatment are that it allows: 1/ the use of the approach in all existing codes based on the Correlated-*k* approach, with only minor modifications, 2/ the building of the clusters for a single reference composition and pressure. The correlation assumption then deals with variations of composition and pressure along heterogeneous paths.

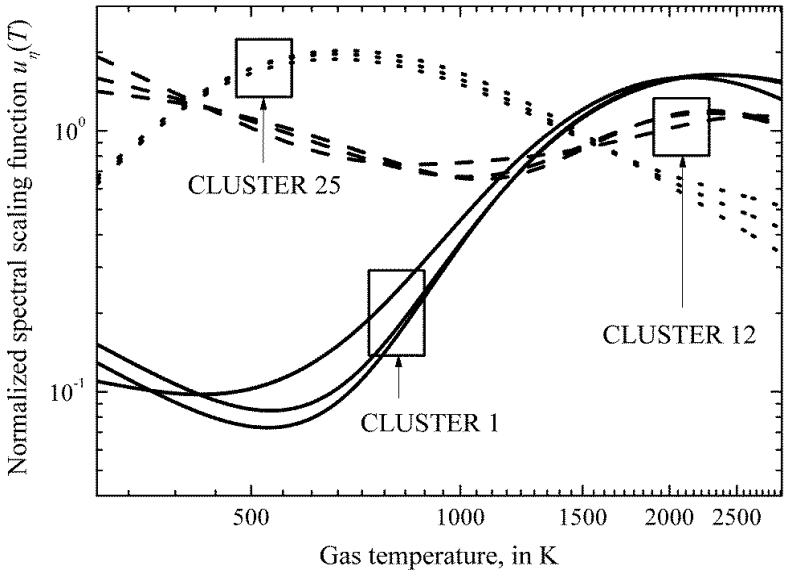

Figure 4. Examples of spectral scaling function for H_2O over the [3287.5 ; 3312.5] cm^{-1} spectral interval. Clusters were obtained with the functional form FF2.

Following Eqs. (32,38), on which the MSF is based, it is clear that the present approach shares many similarities with other existing models. In fact, any number of scaling functions can be used in Eq. (32). Let us thus consider a LBL spectrum calculated at high resolution and write N the number of points for which the absorption coefficient was evaluated inside $\Delta\eta$. Several cases can be considered:

- If $P = N$, then MSF model and LBL calculation are rigorously the same.
- If $P = 1$, then the combination of Eqs. (32,38) provides the so-called scaled-k model [14].
- If scaling functions are built in such a way that they associate the same value of $\hat{u}_p\left(\underline{\phi}\right)$ to all the wavenumbers that correspond to a given value k_p of the absorption coefficient in the reference state, viz.: if $\kappa_\eta\left(\underline{\phi}^{ref}\right) = k_p \Rightarrow \hat{u}_p\left(\underline{\phi}\right) = \kappa_\eta\left(\underline{\phi}\right) / \kappa_\eta\left(\underline{\phi}^{ref}\right) = u_p\left(k_p, \underline{\phi}\right)$, then we define a relationship between the gas spectra in the two states that can be written in the following form: $\kappa_\eta\left(\underline{\phi}\right) = u_p\left(k_p, \underline{\phi}\right) \cdot \kappa_\eta\left(\underline{\phi}^{ref}\right) = h\left[\kappa_\eta\left(\underline{\phi}^{ref}\right)\right]$ where h is a function that correlates explicitly the values of the absorption coefficients in the two states: this provides exactly the correlated-k model [14]. However, no restriction about the behavior, monotonous or not, of the correlating function is then introduced.
- Theoretical links between MS and Fictitious gas approaches are discussed in Appendix.
- If sub-spectral intervals are built by grouping together wavenumbers associated to similar scaling functions, then: 1/ if scaling functions are defined explicitly by a given prescribed functional form, MSF provides the so-called multi-group approach described in Refs. [20,21] when the same basis of functions as proposed in these references are used, 2/ if those scaling functions are defined implicitly, viz. without explicit functional form but in terms of their overall behavior (ie. increase or decrease over the whole set of thermophysical states, or increase and then decrease, etc), the MSF provides the multi-group approach described in Refs. [22,23].
- If $P = 1$ and if we assume that the k-distribution function is Inverse Gaussian, we finally end up with the SNB Malkmus' model together with the Curtis-Godson approximation (this can be readily shown by considering the solutions of Eq. (38) for the scaling function at the optically thin and thick limits, that provide in this case analytical solutions, and then by reporting the results inside Eq. (32) written over a non-uniform path).

In other words, the set of Eqs. (32,38) provides the most general approximate model for gas radiation in non-uniform media. All existing models can thus be obtained by different ways to approximate the exact formula set by Eqs. (20,22).

5. Applications

5.1. Preliminary comments

All results provided in this section correspond to mixtures of H_2O and N_2. Reference LBL spectra were calculated using the HITEMP2010 [24] spectroscopic database for 27 temperature values between $T_{\min}$ = 300 K and $T_{\max}$ = 2,900 K and molar fractions x_{H_2O} = 0.01, 0.1, 0.2, 0.4, 0.6, 0.8 and 1.0. The total pressure is 1 atm. More details about those calculations can be found in Ref. [25]. The only differences in the present work are that: 1/ total partition sums were calculated using the polynomial formulas given in Ref. [26], 2/ the distances from line centers for the estimation of Lorentz profiles were taken from Ref. [27], 3/ the data used for the calculation of the Lorentz HWHM of the spectral lines where those given in the HITEMP2010 database.

Once LBL data are available, spectral groups (clusters) are built following the method described in section 4.2. (As said in section 4.3, clusters can be made using a reference pressure and composition. Here, values P^{ref} = 1 atm and $x_{H_2O}^{ref}$ = 0.1 were chosen). A detailed analysis of those sets of wavenumbers has shown that the clusters are mostly independent on the choice of the Functional Form FF1 or FF2. This was confirmed by several test cases (not given here) where the two models were found to provide results within ~0.1% on narrow band calculations. Accordingly, only the model based on FF2 will be considered here and will be referred to as MSC*k*.

Four approximate models are considered for comparisons with LBL reference data: C*k*-25, which is the usual narrow band C*k* model averaged over 25 cm^{-1} spectral intervals [1]; C*k*-1, the C*k* model with data generated at 1 cm^{-1}; MSC*k* with functional forms FF2 with p = 25 (distinct scaling functions); and *k*-Map (only for 0D test cases) viz. based on a direct application of Eqs. (20,21). To ensure fair comparison among the four models, results were averaged over 25 cm^{-1}. Notice that C*k*-1 and MSC*k* models share the same computational cost, but use different discretizations of the narrow bands.

The building of those model parameters was done by using the same method as described in Ref. [8]. This approach requires defining a reference temperature. Here we have chosen T^{ref} = 2,900 K (this value, together with P^{ref} = 1 atm and $x_{H_2O}^{ref}$ = 0.1 chosen previously, defines our reference state). 15 values of k^{ref} were used to discretize the interval $\left[k_{\min}^{ref}, k_{\max}^{ref}\right]$. Those minimum and maximum values of the absorption coefficient in the reference state were taken directly from the LBL dataset. Then, the corresponding values of absorption coefficient in all the other thermophysical states were obtained by solving Eq. (39).

In the next section, 0D test cases only involve two distinct thermophysical states. Notice that for these cases, *k*-Map uses 15^2 values of *k*. 1D calculations were performed using the semi-analytical method described in Ref. [28].

5.2. Examples of applications in 0D and 1D geometries

To illustrate the validity of the various models considered in this work, we first consider two simple 0D examples taken from Ref. [14]. In these cases, a slab of hot gas (at 1,000 K or 2,000 K) radiates through a cold slab at 300 K. Both layers have the same length (50 cm). The total pressure is 1 atm and the molar fractions of H_2O (x_{H_2O} = 0.2) are the same in both slabs. Results, in terms of emissivities as defined by Modest in Ref. [14], are depicted in figure 5 (T_h = 1,000 K) and figure 6 (T_h = 2,000 K). The C*k*-25 model provides in both cases the worst results, with errors that reach 55% when compared to the reference LBL data. Those results are consistent with those reported in Ref. [14]. The C*k*-1 model is more accurate, but errors up to 20% are observed. Significant improvements can be obtained with the MSC*k* and *k*-Map models for which errors do not exceed 4.2% for MSC*k* and 2.2% for *k*-Map in the worst cases. The *k*-Map approach is slightly more accurate than MSC*k* with a band averaged

(over the 1000-2500 cm^{-1} spectral interval) error that is lower than 0.11%, compared to an error of up to 1.2% for MSC*k*.

The third test case was taken from Ref. [3]. It corresponds to a 1D triangular temperature profile: the temperature is constant and equal to the wall temperature T_w=500 K except at the centre of the domain where it increases up to 2,500 K inside a layer of width 10 cm. The gas is homogeneous (x_{H_2O} = 0.1) and the total pressure is 1 atm. Results for this case, which are provided in terms of the total net flux as a function of the distance between the walls, are depicted in figure 7. Again, the MSC*k* model clearly outperforms more conventional C*k* approaches. Furthermore, if we compare the order of magnitude of the errors on wall fluxes obtained here with those given in Ref. [3] (see figure 7 in this reference), it appears that the MSC*k* and Fictitious Gases (FG) approaches provide in this case very similar accuracies. This is not really surprising because, as shown for instance in Appendix, FG and MS techniques share many similarities. Nevertheless, one of the advantages of MSC*k* over CKFG is that CKFG approach is usually applied in terms of transmissivity (when formulated in terms of absorption coefficients, its computational cost is higher than a LBL calculation). Therefore, it cannot be used when the gas is surrounded by reflecting walls [3]. The MSC*k* method, on the other hand, does not suffer from the same possible source of error because, over clusters, the gas radiation model reduces to a usual correlated-*k* model, known to be applicable with non-black boundaries. Furthermore, for the same reason, MSC*k* can be applied in uniform media without any loss of accuracy, which may not be the case with the CKFG model (see for instance [3]).

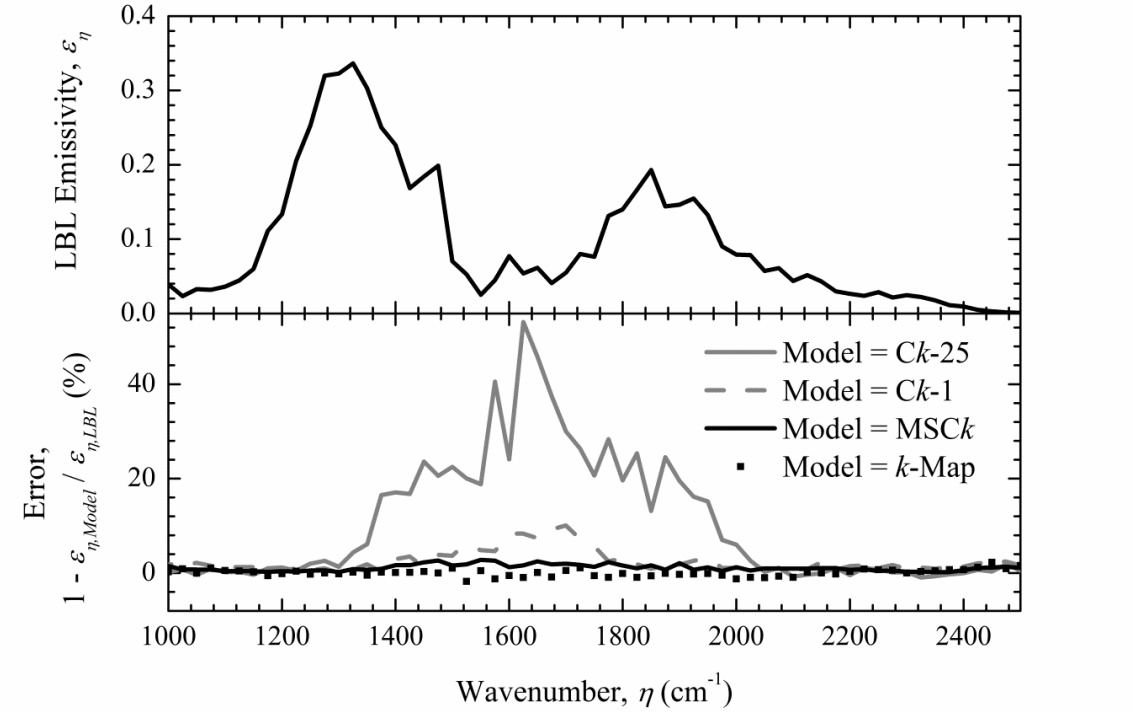

Figure 5. Narrow band emissivities for the 6.3 μm band of H_2O calculated by the LBL (top) method and errors due to the use of C*k*-25, C*k*-1, MSC*k* and *k*-Map approximate models. T_h = 1,000 K.

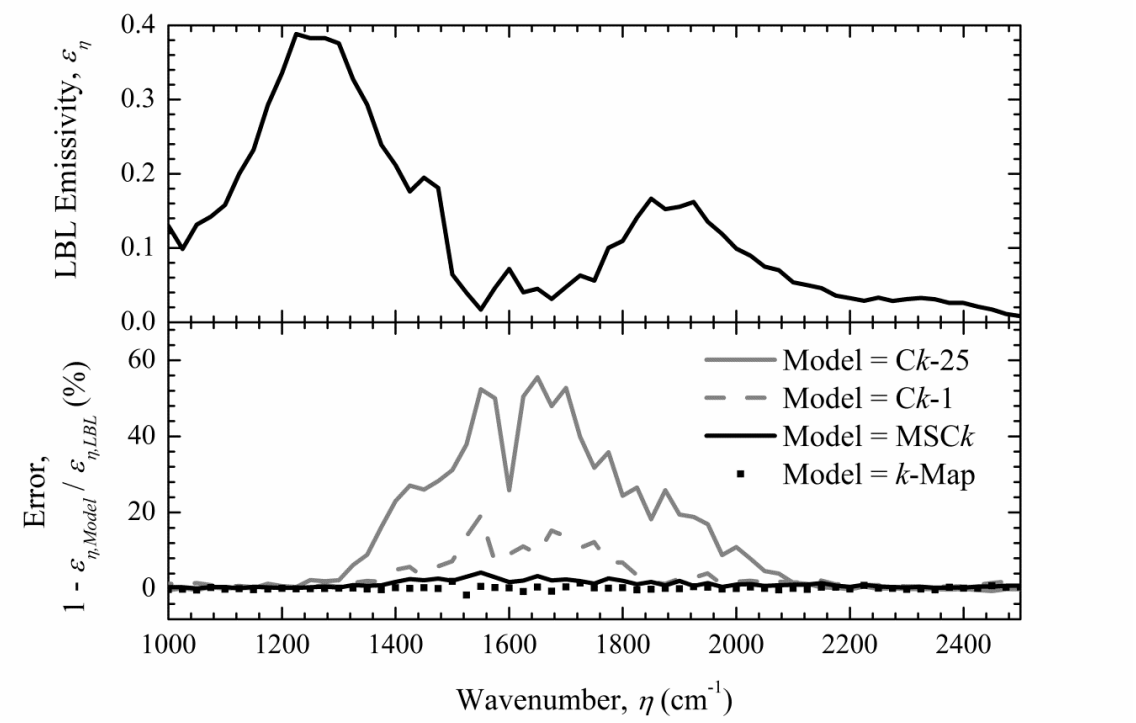

Figure 6. Narrow band emissivities for the 6.3 μm band of H_2O calculated by the LBL (top) method and errors due to the use of C*k*-25, C*k*-1, MSC*k* and *k*-Map approximate models. T_h = 2,000 K.

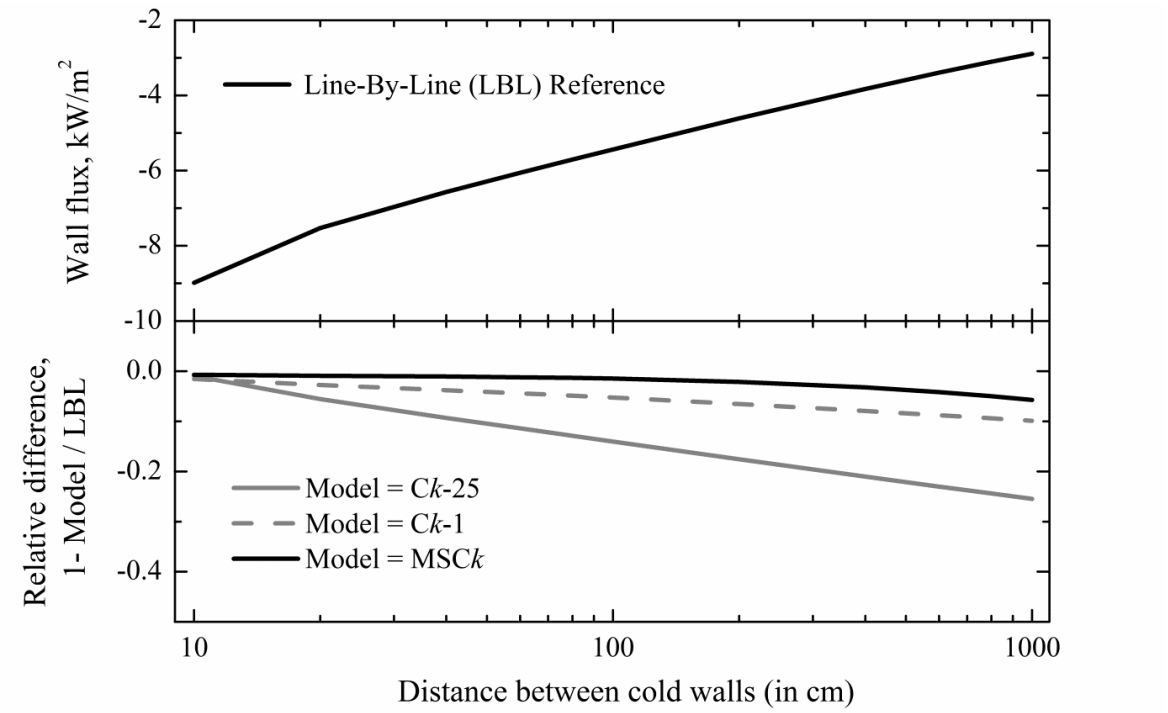

Figure 7. Wall net flux for a triangular temperature profile (from Ref. [3]) – the gas (H_2O-N_2 mixture, x_{H_2O} = 0.1, P = 1 atm) is surrounded by cold black walls at 500 K. Top: wall net flux calculated LBL, bottom: relative difference between model and LBL calculations. The hot layer thickness is 10 cm.

6. Conclusion

A general formula for the application of *k*-distribution approaches in non-uniform gaseous media was proposed, together with a simpler and computationally more efficient technique (based on the so-called Multi-Spectral Framework (MSF)) to allow its application in radiative heat transfer. Both models (the exact approach called *k*-Map, and its approximation, MSC*k*) were assessed against LBL reference data for H_2O-N_2 mixtures in 0D geometries. For 1D geometries, the exact approach cannot be recommended due to its computational cost, and in this case the use of the MSC*k* model is appropriate. Those two approaches were found to outperform usual *k*-distribution techniques in several test cases taken from the literature. Further developments, planned as future work, are still required to optimize the MSC*k* model (in terms of the number of values of *k* required for the calculation of *k*-integrals, and in terms of the optimal number of clusters) for application in radiative heat transfer. The application of the proposed method over the full spectrum will also be studied.

Acknowledgments

This work was supported by the French National Research Agency under the grant ANR-12-BS09-0018 SMART-LECT.

Appendix. Functional *k*-distribution formulation

We consider a narrow band $\Delta\eta$. Over this interval, the spectral absorption coefficient is the sum of the contributions of N_l spectral lines (whose centers may be inside or outside $\Delta\eta$). Each line corresponds to a radiative transition between two energy states of the molecules. Let us write E_l the lowest value of energy for the *l*-th spectral line. It is possible to assemble the spectral lines into *N* groups (equivalent to fictitious gases) with the same value of parameter E_l. If all spectral lines are associated to distinct values of E_l, then $N = N_l$. More generally, $N \le N_l$.

Let us assume that for any wavenumber $\eta \in \Delta\eta$, the spectral absorption coefficient of the gas in a thermophysical state given by the state vector $\underline{\phi}$ (temperature *T*, composition *x* and total pressure *P*) can be written as the sum of N scaled spectra, viz.

$$\kappa_\eta\left(\underline{\phi}\right) = \kappa_{\eta,1}\left(\underline{\phi}^{ref}\right)\cdot e_1'\left(\underline{\phi}\right) + \kappa_{\eta,2}\left(\underline{\phi}^{ref}\right)\cdot e_2'\left(\underline{\phi}\right) + ... + \kappa_{\eta,N}\left(\underline{\phi}^{ref}\right)\cdot e_N'\left(\underline{\phi}\right) \qquad \text{(A.1)}$$

where $\underline{\phi}^{ref}$ represents a reference state and $e_i'\left(\underline{\phi}\right)$, $i = 1,..,N$ the scaling functions. The corresponding temperature, T^{ref}, is chosen here equal to $T_{\min}$.

This statement is equivalent to assume that the profiles associated to the spectral lines that appear in the spectrum (that are here assumed to be Lorentzian) are scaled. This approximation was used in Ref. [6] to introduce the Fictitious gases approach. It was justified as follows: at low resolution, line-wings have a more important impact that line centers. Accordingly one can assume, as a first approximation, that line profiles are scaled viz.

$$\begin{aligned} f_L\left(\eta-\eta_l,\underline{\phi}\right) &= \frac{\gamma_L\left(\underline{\phi}\right)}{\pi}\frac{1}{\left[\gamma_L\left(\underline{\phi}\right)\right]^2+\left(\eta-\eta_l\right)^2} = \frac{\gamma_L\left(\underline{\phi}\right)}{\gamma_L\left(\underline{\phi}^{ref}\right)}\frac{\gamma_L\left(\underline{\phi}^{ref}\right)}{\pi}\frac{1}{\left[\gamma_L\left(\underline{\phi}\right)\right]^2+\left(\eta-\eta_l\right)^2} \\ &\approx \frac{\gamma_L\left(\underline{\phi}\right)}{\gamma_L\left(\underline{\phi}^{ref}\right)}\frac{\gamma_L\left(\underline{\phi}^{ref}\right)}{\pi}\frac{1}{\left[\gamma_L\left(\underline{\phi}^{ref}\right)\right]^2+\left(\eta-\eta_l\right)^2} \\ &= \frac{\gamma_L\left(\underline{\phi}\right)}{\gamma_L\left(\underline{\phi}^{ref}\right)} f_L\left(\eta-\eta_l,\underline{\phi}^{ref}\right) \end{aligned} \qquad \text{(A.2)}$$

where η_l is the center of the *l*-th line, γ_L the half-width at half-maximum of the Lorentz profile assumed to be the same for all spectral lines, f_L the Lorentz profile and $\underline{\phi}$ the state vector as defined previously. γ_L is usually (see for instance Ref. [29]) estimated as the product of a function of temperature, $\gamma_{L,T}(T)$, and a function of composition, $\gamma_{L,c}(x,P)$:

$$\gamma_L\left(\underline{\phi}\right)=\gamma_{L,T}(T)\ \gamma_{L,c}(x,P) \tag{A.3}$$

Furthermore, we assume that: 1/ all spectral lines share the same partition function $Q(T)$, 2/ all terms of the form $1-exp\left(-hc\eta_l/k_BT\right)$ (that appear in the calculation of linestrengths) can be approximated as $1-exp\left(-hc\bar{\eta}/k_BT\right)$ where $\bar{\eta}$ represents the band center and k_B is the Boltzman's constant. Then we can write functions $e_i'\left(\underline{\phi}\right)$, $i=1,..,N$ explicitly:

$$\begin{aligned} e_i'\left(\underline{\phi}\right) &= \underbrace{\frac{1-exp\left(-hc\bar{\eta}/k_BT\right)}{1-exp\left(-hc\bar{\eta}/k_BT^{ref}\right)}\frac{Q\left(T^{ref}\right)}{Q(T)}\frac{T^{ref}}{T}}_{v(T)}\underbrace{\frac{\gamma_{L,T}(T)}{\gamma_{L,T}\left(T^{ref}\right)}}_{G_T(T)}\underbrace{\frac{\gamma_{L,c}(x,P)}{\gamma_{L,c}\left(x^{ref},P^{ref}\right)}}_{G_c(x,P)}\underbrace{exp\left[-\frac{E_i}{k_B}\left(\frac{1}{T}-\frac{1}{T^{ref}}\right)\right]}_{e_i(T)} \\ &= v(T)\cdot G_T(T)\cdot G_c(x,P)\cdot e_i(T) \end{aligned} \tag{A.4}$$

As $v(T)G_T(T)\neq 0$, it is possible to reformulate Eq. (A.1) into:

$$\begin{cases} \kappa_\eta\left(\underline{\phi}\right)=\dfrac{\kappa_\eta\left(x^{ref},P^{ref},T\right)}{v(T)G_T(T)}\times v(T)G_T(T)\times G_c(x,P) \\ \dfrac{\kappa_\eta\left(x^{ref},P^{ref},T\right)}{v(T)G_T(T)}=\kappa_{\eta,1}\left(\underline{\phi}^{ref}\right)\cdot e_1(T)+\kappa_{\eta,2}\left(\underline{\phi}^{ref}\right)\cdot e_2(T)+...+\kappa_{\eta,N}\left(\underline{\phi}^{ref}\right)\cdot e_N(T) \end{cases} \tag{A.5}$$

where:

$$e_i(T)=exp\left[-\frac{E_i}{k_B}\left(\frac{1}{T}-\frac{1}{T^{ref}}\right)\right] \tag{A.6}$$

In Eq. (A.5), $\kappa_\eta\left(x^{ref},P^{ref},T\right)$ represents the spectral absorption coefficient at temperature *T*, composition x^{ref} and total pressure P^{ref}.

Now, let us consider the set of temperature T_j, $j=1,..,N$ defined as:

$$\frac{1}{T_j}-\frac{1}{T^{ref}}=\frac{j-1}{N-1}\left(\frac{1}{T_{\max}}-\frac{1}{T_{\min}}\right) \tag{A.7}$$

We can then use (A.5) to set the linear system of equations:

$$\boldsymbol{k}=J_\Phi\boldsymbol{K}\ \Leftrightarrow\ \boldsymbol{K}=J_\Phi^{-1}\boldsymbol{k} \tag{A.8}$$

where $\boldsymbol{k}$ and $\boldsymbol{K}$ are the vectors of components $[\boldsymbol{k}]_i=\kappa_\eta\left(x^{ref},P^{ref},T_i\right)\Big/\left[v(T_i)G_T(T_i)\right]$ and $[\boldsymbol{K}]_i=\kappa_{\eta,i}\left(\underline{\phi}^{ref}\right)$ respectively. J_Φ is a N by N square invertible matrix (with the set of temperatures given by Eq. (A.7), this matrix is of the Vandermonde type which is here invertible because all E_i's are distinct). Mathematically, Eq. (A.8) represents a change of basis and J_Φ is the corresponding

Jacobian matrix whose coefficients are: $\left[J_\Phi\right]_{ij} = \dfrac{\partial\left[\kappa_\eta\left(x^{ref},P^{ref},T_i\right)/\nu\left(T_i\right)G_T\left(T_i\right)\right]}{\partial\kappa_{\eta,j}\left(\underline{\phi}^{ref}\right)} = e_j\left(T_i\right)$. In this case, the set $e_1(T),..,e_N(T)$ defines a basis of a space $H\left(e_1,..,e_N\right)$ of functions $f(T)$ over the interval $T\in\left[T_{\min},T_{\max}\right]$:

$$H\left(e_1,..,e_N\right)=\left\{\begin{array}{c}\text{functions K}:\left[T_{\min},T_{\max}\right]\to\mathbb{R}\text{ such that}\\ \mathrm{K}(T)=\nu(T)G_T(T)\sum_{j=1}^{N}a_j\ e_j(T),\ \forall\left(a_1,..,a_N\right)\in\mathbb{R}^N\end{array}\right\} \tag{A.9}$$

Now, using Eq. (A.5), the band averaged transmission function of a path of length *L* inside the gas in any thermophysical condition $\underline{\phi}$ can be written as the multiple integral:

$$\tau^{\Delta\eta}(L)=\underbrace{\int_0^{+\infty}\int_0^{+\infty}...\int_0^{+\infty}}_{N\text{ integrals}}\exp\left\{-xP\ \nu(T)G_T(T)\ G_c\left(x,P\right)\left[K_1\cdot e_1(T)+...+K_N\cdot e_N(T)\right]L\right\}d\tilde{g}_N\left(K_1,..,K_N\right) \tag{A.10}$$

where:

$$\tilde{g}_N\left(K_1,..,K_N\right)=\frac{1}{\Delta\eta}\int_{\Delta\eta}H\left[K_1-\kappa_{\eta,1}\left(\underline{\phi}^{ref}\right)\right]...H\left[K_N-\kappa_{\eta,N}\left(\underline{\phi}^{ref}\right)\right]d\eta \tag{A.11}$$

Let us write β_{ij} the elements of the inverse of matrix J_Φ: $\left[J_\Phi^{-1}\right]_{ij}=\beta_{ij}$.

We have, following (A.8):

$$\begin{aligned}K_1\cdot e_1(T)+...+K_N\cdot e_N(T)&=\left(\sum_{i=1}^{N}\beta_{1i}k_i\right)\cdot e_1(T)+...+\left(\sum_{i=1}^{N}\beta_{Ni}k_i\right)\cdot e_N(T)\\&=k_1.\underbrace{\sum_{j=1}^{N}\beta_{j1}e_j(T)}_{\xi_1(T)}+...+k_N.\underbrace{\sum_{j=1}^{N}\beta_{jN}e_j(T)}_{\xi_N(T)}\end{aligned} \tag{A.12}$$

and, formally, from Ref. [13]:

$$\begin{aligned}\frac{\partial^N\tilde{g}_N\left(K_1,..,K_N\right)}{\partial K_1..\partial K_N}&=\frac{1}{\Delta\eta}\int_{\Delta\eta}\delta\left[K_1-\kappa_{\eta,1}\left(T^{ref}\right)\right]...\delta\left[K_N-\kappa_{\eta,N}\left(T^{ref}\right)\right]d\eta\\&=\left|det\,J_\Phi\right|\ \frac{1}{\Delta\eta}\int_{\Delta\eta}\delta\left[k_1-\frac{\kappa_\eta\left(x^{ref},P^{ref},T_1\right)}{\nu(T_1)G_T(T_1)}\right]...\delta\left[k_N-\frac{\kappa_\eta\left(x^{ref},P^{ref},T_N\right)}{\nu(T_N)G_T(T_N)}\right]d\eta\\&=\left|det\,J_\Phi\right|\ \frac{\partial g_N^{\nu}\left(k_1,..,k_N\right)}{\partial k_1...\partial k_N}\end{aligned} \tag{A.13-a}$$

where:

$$g_N^{\nu}\left(k_1,..,k_N\right)=\frac{1}{\Delta\eta}\int_{\Delta\eta}H\left[k_1-\frac{\kappa_\eta\left(x^{ref},P^{ref},T_1\right)}{\nu(T_1)G_T(T_1)}\right]...H\left[k_N-\frac{\kappa_\eta\left(x^{ref},P^{ref},T_N\right)}{\nu(T_N)G_T(T_N)}\right]d\eta \tag{A.13-b}$$

This yields:

$$\tau^{\Delta\eta}(L)=\underbrace{\int_0^{+\infty}\int_0^{+\infty}\ldots\int_0^{+\infty}}_{N\text{ integrals}}\exp\left\{-xPL\ v(T)G_T(T)\ G_c(x,P)\left[k_1\cdot\mathcal{E}_1(T)+\ldots+k_N\cdot\mathcal{E}_N(T)\right]\right\}\ dg_N^v(k_1,..,k_N) \tag{A.14}$$

Accordingly, formulas (A.10) and (A.14) are rigorously equivalent. They can be both written formally in functional integral forms (so as to simplify the notations):

$$\begin{cases}\tau^{\Delta\eta}(L)=\displaystyle\int_{\mathrm{K}(T)\in H(e_1,..,e_N)}\exp\left[-xPG_c(x,P)\ \ \mathrm{K}(T)L\right]dW\left[\mathrm{K}(T)\right]\\ \tau^{\Delta\eta}(L)=\displaystyle\int_{\kappa(T)\in H(\mathcal{E}_1,..,\mathcal{E}_N)}\exp\left[-xPG_c(x,P)\ \ \kappa(T)L\right]dw\left[\kappa(T)\right]\end{cases} \tag{A.15}$$

where $dW\left[\mathrm{K}(T)\right]=d\tilde{g}_N(K_1,..,K_N)$, $dw\left[\kappa(T)\right]=dg_N^v(k_1,..,k_N)$ and where we define the following space of functions:

$$H(\mathcal{E}_1,..,\mathcal{E}_N)=\left\{\begin{array}{c}\text{functions }\kappa:[T_{\min},T_{\max}]\to\mathbb{R}\text{ such that}\\ \kappa(T)=v(T)G_T(T)\cdot\displaystyle\sum_{j=1}^{N}a_j\mathcal{E}_j(T),\ \forall(a_1,..,a_N)\in\mathbb{R}^N\end{array}\right\} \tag{A.16}$$

In Eq. (A.15), $dW\left[\mathrm{K}(T)\right]=d\tilde{g}_N(K_1,..,K_N)$ defines a measure on the space of functions $H(e_1,..,e_N)$. Similarly, $dw\left[\kappa(T)\right]=dg_N^v(k_1,..,k_N)$ is a measure on $H(\mathcal{E}_1,..,\mathcal{E}_N)$. Eq. (A.15) can be compared to the more usual formulas Eqs. (1,2). That becomes what can be called a functional *k*-distribution formulation.

Formulas (A.15) can be obviously extended to non-uniform media. Nevertheless, those formulations do not have (*a priori*) a real benefit over Eq. (20) for applications in radiative heat transfer. Indeed, most problems are typically formulated in terms of discretized temperature fields (viz. values of temperatures at discrete points sampled through a mesh). In those applications, Eq. (20) provides the exact solution. Nevertheless, this formulation is interesting from a fundamental point of view because:

- it noticeably exhibits the links that exist between *k*-distributions in non-uniform media and functional data concepts and methods (such as FDA), as used in the multispectral approach.
- it clearly shows that LBL and Fictitious gas methods (which are mainly founded on the first integral formulation in Eq. (A.15)) and mapping techniques (based on the second formula in the same set of equations) are rigorously equivalent.

Finally, it should be noticed that the problem usually encountered for the definition of a measure in functional or path integration (see for instance the discussion pages 4-5 in Ref. [30] - the same problem is found in Functional Data Analysis, [31]) is avoided here because the spaces of functions considered for the calculation of the integrals are of finite dimensions N (that represents the number of spectra that can be associated to distinct values of E_i that one can find in the spectroscopic database - this number is always finite). Over those spaces, a measure can be defined in terms of the components of any function in the basis $e_1(T),..,e_N(T)$ or $\mathcal{E}_1(T),..,\mathcal{E}_N(T)$. This may not be the case in a general frame [32].

References

[1] Modest MF 2003 *Radiative heat transfer* (New York: Academic Press)
[2] Goody RM, Yung YL 1989 *Atmospheric radiation - theoretical basis* (New York: Oxford University Press)

[3] Pierrot L, Rivière Ph, Soufiani A, Taine J 1999 *J. Quant. Spectr. Rad. Transfer* **62** 523-548
[4] Modest MF, Zhang H 2003 *J. Heat Transfer* **124** 30-38
[5] Denison MK, Webb BW 1993 *J. Heat Transfer* **115** 1004-1012
[6] Levi di Leon R, Taine J 1986 *Rev. Phys. Appl.* **21** 825-831
[7] West R, Crisp D, Chen L 1990 *J. Quant. Spectr. Rad. Transfer* **43** 191-199
[8] André F, Hou L, Roger M, Vaillon R 2014 *J. Quant. Spectr. Rad. Transfer* **147** 178-195
[9] Ambartzumian V 1934 *Publ Obs Astron Univ Leningrad* **6** 7-18
[10] Lebedinski AI 1939 *Proc Leningrad Univ Ser Math* **3(31)** 152-75
[11] Kondratiev KY 1969 *Radiation in the atmosphere* (New York: Academic Press)
[12] Arking A, Grossman K 1972 *J Atmos Sci* **29** 937-949
[13] Kanwal R 1998 *Generalized functions: theory and practice* (Boston: Birkhäuser)
[14] Modest MF 2003 *J. Quant. Spectr. Rad. Transfer* **76** 69-83
[15] Abramowitz M, Stegun IA 1965 *Handbook of Mathematical Functions* (Dover)
[16] Everitt BS, Landau S, Leese M, Stahl D 2011 *Cluster analysis* (John Wiley and Sons)
[17] Ramsay JO, Silverman BW 2005 *Functional data analysis* (Springer series in statistics)
[18] Jacques J, Preda C 2013 *Functional data clustering: a survey* Research Report N°8198
[19] Ferreira L, Hitchcock DB 2009 *Communications in Statistics* **38** 1925-1949
[20] Zhang H, Modest MF 2002 *J. Quant. Spectr. Rad. Transfer* **73** 349-360
[21] Zhang H, Modest MF 2003 *J. Heat Transfer* **125** 454-461
[22] Pal G, Modest MF, Wang L *J. Heat Transfer* **130** 082701-082708
[23] Pal G, Modest MF *J. Heat Transfer* **132** 023307-1-023307-9
[24] Rothman LS, et al 2010 *J. Quant. Spectr. Rad. Transfer* **111** 2139-2150
[25] Andre F, Vaillon R 2010 *J. Quant. Spectr. Rad. Transfer* **111** 1900-1911
[26] Vidler M, Tennyson J 2000 *J Chem Phys* **113** 9766-9771
[27] Riviere P, Soufiani A 2012 *Int. J. Heat Mass Transfer* **55** 3349-3358
[28] Solovjov VP, Webb BW 2008 *J. Quant. Spectr. Rad. Transfer* **109** 245-257
[29] Rothman LS, et al 1998 *J. Quant. Spectr. Rad. Transfer* **60** 665-710
[30] Chaichian M, Demichev A 2001 *Path integrals in Physics Volume I Stochastic processes and quantum mechanics* (Bristol and Philadelphia: IOP)
[31] Delaigle A, Hall P 2010 *Annals Stat* **38** 1171-1193
[32] Menskii MB 1992 *Theoretical and Math Phys* **93** 1262-1267